Fire Safety Journal 91 (2017) 653–661

Contents lists available at ScienceDirect

Fire Safety Journal

journal homepage: www.elsevier.com/locate/firesaf

IAFSS 12th Symposium 2017

Measuring fuel transport through fluorocarbon and fluorine-free firefighting foams

Katherine M. Hinnant, Spencer L. Giles, Ramagopal Ananth*

Chemistry Division/Combustion Dynamics and Modeling, U.S. Naval Research Laboratory, 4555 Overlook Ave SW, Washington, D.C. 20375, United States

ARTICLE INFO

Keywords:
Fire suppression
Fuel transport
Fluorinated foams
Fluorine-free foams
Film formation
Solubility

ABSTRACT

A flux chamber was designed to measure the transient fuel transport through a foam layer before significant degradation of foam occurred. The fuel transport rate through AFFF (fluorinated foam) was much slower than through RF6 (fluorine-free foam) with break-through times being 820 s and 276 s respectively over n-heptane. The fuel flux through AFFF covering three fuel pools (n-heptane, iso-octane, and methyl-cyclohexane) was also measured. AFFF had the smallest flux over iso-octane with a break-through time over 1900 s and the highest flux over methyl-cyclohexane with a break-through time under 80 s even though the fuels have similar vapor pressures at room temperature. Despite the lack of aqueous film formation on an iso-octane fuel pool, the fuel vapor flux through AFFF was much smaller relative to the methyl-cyclohexane pool, which enables film formation due to its higher surface tension than iso-octane. Our measurements of transient fuel flux show that the foam layer is a significant barrier to fuel vapor transport. The data suggest a transient mechanism based on the suppression of fuel adsorption onto bubble lamellae surfaces due to the oleophobicity of fluorocarbon surfactants, which is consistent with fuel solubility data. This suggests that surfactants that suppress fuel adsorption and solubility into bubble lamellae surfaces may reduce fuel transport through foams.

1. Introduction

Liquid pool fires are suppressed by using aqueous foams in both military and civilian applications worldwide. Aqueous film forming foam (AFFF) is considered the most effective liquid pool fire suppressant because of its fast fire extinction and protection against re-ignition of the fuel pool [1]. Although the fire suppression capabilities of AFFF have passed stringent fire extinction requirements of U.S. Navy Military Standard (MilSpec) testing [2], foam solutions have been continuously reformulated to address U.S. EPA restrictions [3] due to the toxicity and environmental persistency of fluorocarbon surfactants contained in the foam solution used to generate AFFF. There is a definite need to eliminate the fluorocarbon surfactants from AFFF formulations to address their environmental impact while maintaining the high firefighting performance required by the MilSpec. Commercial fluorine-free foams such as RF6 resulted in significant loss of fire suppression during MilSpec testing [4]. Fire suppression occurs because the foam blocks the fuel vapor transport from the pool surface into the fire, thereby starving the fire to extinction [5]. In this paper, we quantify the relative permeation rates of fuel transport through commercially available AFFF and a fluorine-free firefighting foam containing only hydrocarbon surfactants. We also evaluate the role of the "aqueous film" and the foam layer as barriers to fuel transport to assist in improving fire suppression performance of environmentally benign firefighting foams.

In liquid pool fires, the liquid fuel evaporates at the pool surface and forms vapor. The fuel vapor continuously diffuses away from the pool surface and feeds the fire above the pool. Foam solution is mixed with air to generate a foam with an expansion ratio (volume of foam/volume of liquid contained in the foam) between 5 and 10 [1,2]. The foam is applied directly and continuously onto the burning liquid fuel surface until the fire is extinguished. As the foam deposits on the pool surface, it floats because its density is smaller than that of the liquid fuel. As the foam layer builds up to a small (1–2 cm) thickness, it spreads and covers the surface of the pool under the influence of gravity. The foam is exposed to fire radiation from the fire above as well as hot liquid fuel below, which can increase foam degradation, liquid drainage, and bubble coarsening in the foam, and influence the fuel transport through the foam [6]. Fuel transport is intrinsically time dependent especially in the time scale of fire extinction (30 s for MilSpec fire extinction test [2]). For the purpose of comparing the fuel transport characteristics intrinsic to foams containing fluorinated and fluorine-free surfactants, we generated the foams using an identical method and performed experiments under the controlled conditions of

* Corresponding author.
E-mail address: Ramagopal.ananth@nrl.navy.mil (R. Ananth).

http://dx.doi.org/10.1016/j.firesaf.2017.03.077
Received 14 February 2017; Accepted 15 March 2017
Available online 08 May 2017
0379-7112/ Published by Elsevier Ltd.

the laboratory. We exposed the foams to fuel pools with comparable vapor pressures (at 25 °C) over a relatively short time period to accurately quantify the transient fuel transport rates, in the absence of a fire.

In addition to the foam layer, fluorocarbon surfactants in AFFF foam solution lower the surface tension (16 dynes/cm) of the foam solution and form an extremely thin “aqueous film” layer between the foam and pool surface despite the solution's higher density than the pool. Bernett et al. [7] and Moran et al. [8] demonstrated the formation of a 47 μm (average) thick “aqueous film” by placing the foam solution on an n-octane fuel pool (5 cm diameter) surface in the absence of a foam. Thicker than 47 μm films led to breaking and sinking of the films to the bottom of the pool. Studies comparing the relative contributions of the foam and “aqueous film” as barriers to fuel transport through AFFF have been lacking. This is important because “aqueous film” formation is very difficult to achieve without the use of fluorocarbon surfactants, and attempts to find fluorine-free AFFFs have had limited success to date [9]. It is also important in view of the widespread assumption that the “aqueous film” forms the main barrier to fuel transport relative to foam to explain the superior fire suppression of AFFF observed in numerous large scale tests [4,10–12]. The “aqueous film” has been deemed necessary for fast fire extinction, so much so that it is a requirement for U.S. MilSpec qualified firefighting foams.

The firefighting community developed a flux chamber to characterize a foam's ability to suppress fuel vapors by determining the rate of fuel transport through a specified thickness of foam covering a liquid pool surface over a long time period (steady-state), without the presence of a fire, at ambient, non-combusting, conditions [13–17]. Schaefer et al. [17], relying on previous designs [13–16], designed a flux chamber to compare the performance of fluorinated and fluorine-free foams, which were generated using a food blender. Schaefer et al.’s results revealed that fluorinated foams had a much smaller fuel flux than fluorine-free foams. They attributed this superior performance of fluorinated foams to both the transport resistance of liquid lamellae (bubble wall) separating adjacent bubbles and to the presence of an “aqueous film” [17].

At the U.S. Naval Research Laboratory, Moran et al. [8] developed a flux chamber to measure fuel transport through the “aqueous film” formed by an AFFF foam solution at different film thicknesses. Their work revealed that the presence of a 47 μm thick “aqueous film” suppresses the fuel vapor concentration by a factor of 20 relative to that over a bare fuel pool surface. We previously [4] reconstructed Moran et al.’s flux chamber but made fuel flux measurements from a foam layer covering an n-heptane pool instead of only the “aqueous film”. We reported the steady state molar flux emanating from the foam surface for fluorinated and fluorine-free foams generated by using the same sparging technique and for different fuels [4].

In the present work, we adapt Moran et al.’s apparatus to measure the transient mass transport flux through a foam/film layer. The Naval Research Laboratory's flux chamber design and experimental method is an improvement over previous flux chamber designs in its ability to create a uniform foam layer without significant degradation for studying the transient fuel transport characteristics of the foams. We quantified fuel flux for AFFF over three fuels: n-heptane, methyl-cyclohexane, and iso-octane. AFFF foam solution was shown not to form a film on iso-octane unlike n-heptane and methyl-cyclohexane [4,8]. These three fuels have similar vapor pressures, but differ in surface tension and solubility in water. The transient fuel transport measurements suggest a mechanism for the surfactant's role in fuel transport through aqueous foams.

2. Approach

We generated AFFF (Buckeye 3%, Buckeye Fire Equipment Company, Inc.) and a fluorine-free foam (RF6 6%, Solberg®, formerly 3M Australia) at small flow rates using a sparging method suitable for our bench-scale experiments rather than the pressurized nozzle used in U.S. MilSpec fire extinction tests. The commercial surfactant formulations were prepared from the concentrates supplied by the manufacturers following recommended procedures. The properties of the surfactant solutions, fuels, and foams were measured and are described below along with the experimental apparatus design and procedure. The gap between the foam surface and the nitrogen source is kept at 1 cm for all experiments to maintain identical stagnation flow mass transport conditions in the flux chamber. Measurements were conducted at room temperature (20 °C) with a relatively thick foam layer (4 cm) so that the changes in foam layer thickness due to degradation during the experiment are relatively small (< 0.5 cm). The two foams were characterized by composition, initial bubble diameter, liquid drainage beneath the foam, and initial expansion ratio all measured immediately after foam generation.

2.1. Foam solutions

The commercial AFFF foam solution used in our experiments has already been MilSpec qualified [2]. The foam solution was prepared by mixing the “concentrate solution” provided by the manufacturer with distilled water at 3% concentration by volume. The concentrate is a mixture of fluorocarbon, hydrocarbon surfactants, solvents, other additives, and water. The commercial fluorine-free surfactant solution, RF6, used in our experiments was approved by the International Civil Aviation Organization (ICAO). It was prepared by mixing RF6 “concentrate solution” provided by the manufacturer with distilled water at 6% concentration by volume. The concentrate solution is made of hydrocarbon surfactants, solvents, a polysaccharide thickener, other additives, and water. The composition of the foam solution is about 98% water for each foam with each foam solution having a surfactant concentration less than 1% by weight [18]. The properties of the solutions are given in Table 1 below. Both solutions have similar densities, but differ significantly in viscosity and surface tension with AFFF having a surface tension of 16.4 mN/m and RF6 having a surface tension of 26.4 mN/m at 25 °C. The surface tensions were measured using a DuNoy ring tensiometer at 25 °C. RF6 does not form an “aqueous film” unlike AFFF because of its higher surface tension.

2.2. Fuels

Three fuels, n-heptane, iso-octane, and methyl-cyclohexane, used in our experiments represent straight chained, branched, and cyclic compounds found in a jet fuel. The fuel properties for these three liquid fuels are detailed in Table 2. Table 2 shows that the vapor pressures differ by less than 15% from that of n-heptane. Iso-octane has the smallest surface tension among the fuels studied and does not allow film formation even for Buckeye 3% AFFF foam solution [4]. However, there is a significant difference in fuel solubility in water among the fuels studied especially between methyl-cyclohexane and iso-octane. The differences in solubility could be important because the fuel solubility is the driving force for fuel mass transport through a foam/film.

2.3. Foam generation and foam properties

Fig. 1 details the foam generation process. 400 mL of foam solution

Table 1
Measured foam solution properties at 25 °C.

Foam Solution	AFFF	RF6
Density (g/mL)	1.03	1.06
Viscosity (cP)	1.20	2.40
Surface Tension (mN/m)	16.40	26.40

Table 2
Fuel properties at 25 °C for n-heptane, iso-octane, and methyl-cyclohexane from the Royal Society of Chemistry and fuel MSDS [19–24].

Fuel	Chemical Formula	Molar Mass (g mol^{-1})	Vapor pressure at 25 °C (mmHg)	Solubility (mg fuel L^{-1} water 25 °C)	Surface Tension (dynes cm^{-3})
N-heptane	C_7H_{16}	100.1	39.8	3.4	19.7
Iso-octane	C_8H_{18}	114.1	40.5	2.4	19
Methyl-cyclo-hexane	C_7H_{14}	98.1	37	14.0	23.4

was placed into a 525 mL, 7.5 cm diameter, plastic container. A sparger with a pore size of 170–210 μm (Ace Glass, 4160-09) made of Pyrex glass was attached to the lid of the plastic container so that the sparger was 3 cm from the bottom of the plastic container, submerged 6 cm in the liquid foam solution, when the system was closed. The porous section of the sparger was 3 cm long, 1 cm in diameter with the remainder of the tube being a glass tube. Humidified nitrogen was fed through the sparger producing foam through a plastic outlet tube attached on the side, near the top, of the foam generator. A nitrogen flow controller (Sierra Instruments 0–2 L, Model number 840-L-2-0V1-SV1-D-V1-S1) was used to maintain a flow rate of 390 mL/min. The nitrogen gas was fed through a second sparger immersed in distilled water to humidify the gas before it entered the foam generator.

Even though the same foam generator described in Fig. 1 was used to form both AFFF and RF6 foam, there can be differences in foam properties due to different surfactant solutions (multi-component) used. We therefore characterized the foam properties of AFFF and RF6 foam. A digital image of foam filled in a rectangular container right after foam generation was taken using a camera. ImageJ software was used to calculate the initial, average, diameter of 300 bubbles from the digital image. The bubble diameter distribution was reported elsewhere [25]. The initial expansion ratio was determined by weighing 250 mL of foam immediately after foam generation and dividing the volume of the foam by the weight of the foam. The liquid drainage with time was also measured soon after foam generation. Foam was placed in a 30.5 cm tall graduated cylinder and the volume of drained water at the base of the cylinder was monitored over time with a camera. The 25% drain time was marked when the amount of liquid reached 25% of the total liquid contained in the foam. The foam properties are tabulated in Table 3 below.

RF6 has 40% larger bubbles than AFFF, but a similar expansion ratio initially. Similar expansion ratios means similar amounts of liquid in each of the foams, but AFFF drains liquid roughly two times faster than RF6 for the foams made at bench-scale. This means that after 10 min, the liquid content of AFFF is significantly smaller than that of RF6 and the trend is expected to continue as time progresses.

Table 3
Measured foam properties of AFFF and RF6 from foam generated using a gas sparger with pore size 170–210 μm.

Foam	AFFF	RF6
Initial bubble diameter (mm)	0.54 ± 0.1	0.7 ± 0.3
Initial expansion ratio	9.6 ± 0.3	10.5 ± 0.4
25% liquid drainage time (s)	300	600

Differences in surfactant type and foam solution composition can lead to differences in foam properties, which may contribute to differences in fuel flux through foams as described later.

2.4. Flux chamber design and system flow diagram

We designed a flux chamber in this work incorporating design elements found in the flux chambers of Schaefer et al. [17] and Moran et al. [8]. The flux chamber designed by Schaefer et al. [17] incorporated a two-part system with a 250 mm diameter base housing containing a 1 cm thick foam layer placed over n-heptane, and a top part. The top part contained nitrogen gas, which was fed through a tube with holes over the foam. Nitrogen swept the fuel vapors from the foam surface out of the flux chamber to a gas chromatograph. The residence time for nitrogen flow in the chamber was relatively long (2.7 min). A stirrer was placed in the top part to mix the gases in the space above the foam continuously subjecting the foam surface to a relatively forceful circulation environment.

At the U.S. Naval Research Laboratory, Moran et al. [8] designed a flux chamber to quantify fuel transport through an “aqueous film” formed over a fuel pool. They placed a porous glass frit disc 1 cm above the surface to create a well-defined stagnation flow of nitrogen gas, which gently swept fuel vapors permeating through the entire film surface. We converted the open-system design of Moran et al. into a closed system and fed all of the gases through an FTIR to increase the sensitivity of flux measurements. We placed a foam layer of specified thickness underneath the porous disc to quantify fuel permeation through foams over long periods of time. However, in this reconstructed apparatus, the gas flow through the chamber was initially exposed to a bare fuel pool before foam was placed on top, which lead to a significant initial fuel concentration in the chamber preventing accurate measurements of transient behavior of the fuel transport.

In the present work, we adapt Moran et al.’s apparatus to measure the transient mass transport flux through a foam layer by introducing fuel and foam in an open-system. We then transition to a closed system during the experiment, prior to the measurement of fuel flux by FTIR. We achieve this by using a two part system similar to Schaefer et al. [17] to introduce fuel and foam without exposing the chamber gases to the bare fuel pool. The two part apparatus enables measurement of the fuel transport during the initial period of foam/fuel interaction (<

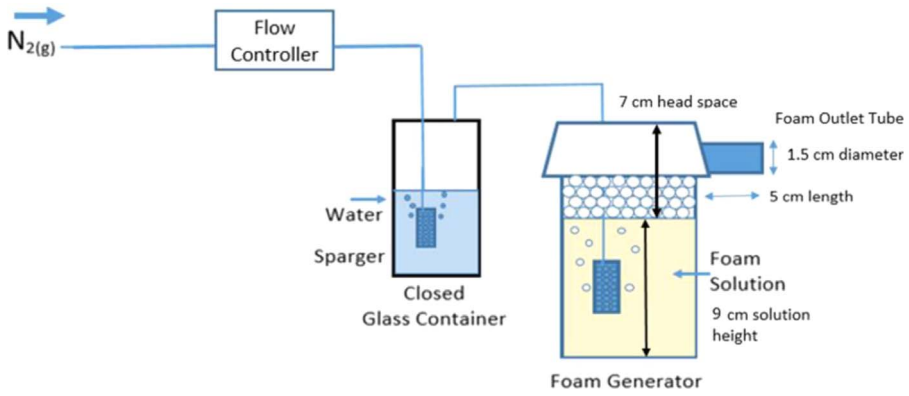

Fig. 1. Diagram of foam generation process.

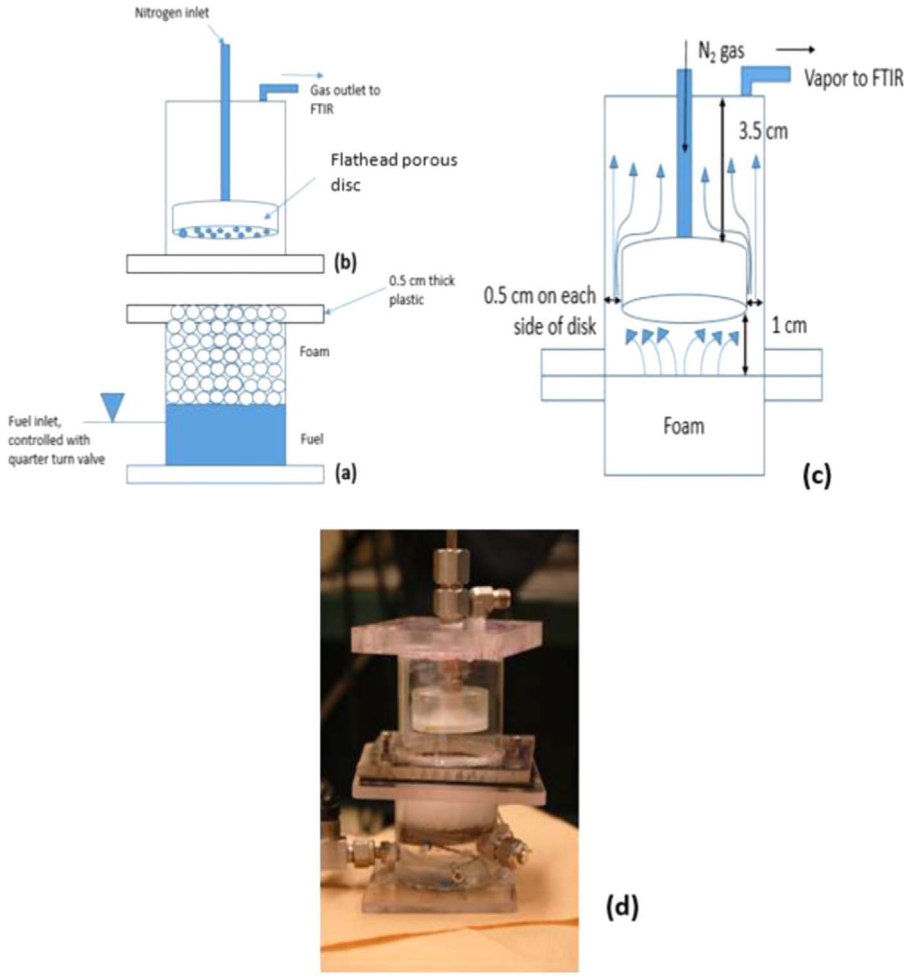

Fig. 2. Flux chamber used to measure fuel transport through foam; (a) bottom part holding the fuel and foam, (b) top part containing the porous disc to sweep gases from the top of the foam, (c) closed-chamber with the stagnation flow streamlines, (d) image of the plexi-glass flux chamber.

45 min) prior to the onset of significant degradation of the foam layer. Initially, the fuel concentration is kept at zero by covering the fuel surface with foam before putting the two parts together to close the flux chamber. We then introduce a sweep gas in a well-defined stagnation flow over the foam layer surface, and accurately measure quantities of fuel vapor over the foam continuously throughout the experiment using an FTIR having a detection limit of 10 ppm.

Fig. 2 shows the flux chamber design used in this work. Fig. 2a is a schematic of the bottom part of the flux chamber while Fig. 2b is a schematic of the top. Fig. 2c is a schematic of the top part of the flux chamber with dimensions and a depiction of stagnation flow and Fig. 2d is a picture of the assembled flux chamber.

Fig. 2a and b are made by cutting a piece of plexi-glass tube, 5.25 cm in inner diameter with 0.5 cm thick walls, into two parts, each 6.5 cm long. One piece was connected to a bottom plexi-glass plate, 0.5 cm in thickness, to close the bottom of the apparatus. A drill press was used to drill a hole into a second plexi-glass plate, 0.5 cm in thickness, slightly larger in diameter than the central cylindrical tube. The drilled plexi-glass was then placed around the tube and sealed on the sides with acrylic adhesive creating the bottom piece shown in Fig. 2a with a sealed bottom and an open top. Two separate holes were drilled into the side of the plexi-glass tube to hold a 1/4th NPT pipe fitting with a quarter turn valve to allow fuel to flow into the bottom of the apparatus and a small hole to hold a thermocouple to measure the fuel pool temperature. Flowing fuel through an inlet at the bottom part of the apparatus instead of pouring the liquid fuel from the top reduced the likelihood of fuel vapors existing above the foam before measurements began. It is important that we have no fuel vapor in the space above the foam initially and the only fuel that appears in that space is due to fuel transport through the foam layer. The second piece of plexi-glass tube had a plexi-glass plate sealed to the top of the tube and a drilled piece sealed to the bottom of the tube creating an open and a closed end as shown in Fig. 2b. Two ¼ in. swagelock fittings were drilled into the closed plexi-glass plate at the top of the tube. One fitting ran a metal tube connected to a porous glass frit disc (2 cm thickness, fine pore size, 10–20 μm) 4 cm in diameter and placed 1 cm above the foam surface.

To connect the upper and lower pieces of the chamber shown in Fig. 2a and b, four holes were drilled into the corners of the drilled plexi-glass plates at the top and bottom of the two separate pieces. A gasket made of rubber was also cut to the diameter of the plexi-glass tube and attached to the drilled plexi-glass plate on the top of the apparatus (b). Small screws were placed in the 4 holes on the top piece (b) and were secured by additional holes in the gasket. When the pieces were to be assembled, the 4 screws on the top piece (b) aligned with the 4 holes on the bottom piece (a). Once the pieces were aligned, 4 clamps were used to secure the 4 sides of the flux apparatus creating an air-tight seal and a closed system. It is important to be able to close the chamber air tight and very quickly, roughly 90 s, to accurately measure the break-through time of fuel vapors through the foam.

Nitrogen was chosen as the carrier gas over air to prevent the formation of a flammable mixture in a closed container. The nitrogen flow was held constant at 234 mL/min using a Sierra instruments (Sierra Instruments 0–500 sccm, Model number 840-L-2-D -S1, 0–

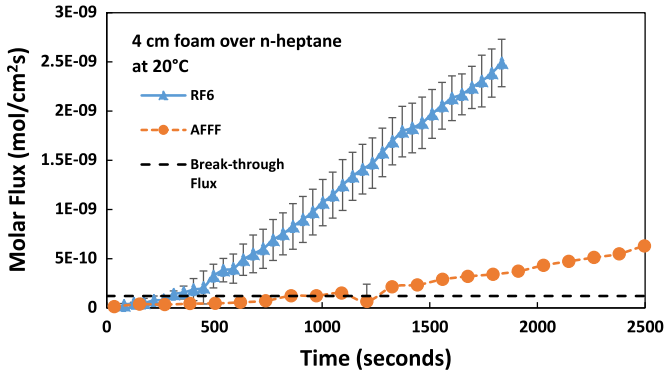

Fig. 3. Measured fuel flux with time through 4 cm thick foam layers covering an n-heptane pool at 20 °C.

500 mL/min) flow controller. A low flow rate was used to ensure that the flow would not deform or interact with the foam layer. All of the nitrogen and the fuel emanating from the foam surface exit the flux chamber. The FTIR is connected to the flux chamber using ¼ in. Teflon tube. Nitrogen flow residence time in the flux chamber is 30 s for the gas volume of 130 cm^3 in the flux chamber. Small nitrogen residence time in the chamber reduces the time lag between FTIR measurements at the outlet of the chamber and the fuel flux emanating from the foam surface.

2.5. Experimental procedure and analysis

To run an experiment, we let the fuel flow by gravity into the bottom part (see Fig. 2a) through a ¼ in. plastic tube connected to the quarter turn valve fitted to a flask containing the liquid fuel. Once the fuel reached an indicated mark on the side of the apparatus, we stopped the fuel flow. This mark indicated the liquid level that would allow room for a 4 cm thick foam in the bottom piece of the apparatus shown in Fig. 2a. Next, foam was generated and allowed to flow directly from the foam generator in Fig. 1 onto the fuel pool in the bottom part of the apparatus. As soon as the foam touched the fuel surface, a timer began. This timer was used to determine the time delay between foam interacting with the fuel and when the FTIR (Midac I series, Model 14001, Serial 587) began recording data. Foam was applied until its upper surface reached the drilled plastic plate on the bottom of the apparatus (Fig. 2a). At this point, a spatula was used to scrape any excess foam from the top, creating a uniform foam layer on top of the fuel. The distance between the glass frit disc to the foam surface was kept constant at 1 cm. The top of the apparatus (Fig. 2b) was then aligned with the bottom, the screws were used to hold the pieces in place and 4 clamps were used to create an air-tight seal. The top of the apparatus was then connected to the FTIR and the timer was stopped and the time recorded. The time delay was on average 70–90 s and was added to the time of the recorded data.

The fuel entering the FTIR was diluted with additional nitrogen through a by-pass tube attached to the FTIR in order to not saturate the gas cell of the FTIR, which is sensitive with a range of 10–2000 ppm for fuels. The FTIR measured the gas sample through a temperature controlled external gas cell. This cell had two inlets and a single outlet with a pressure transducer to monitor the pressure inside the cell. One inlet to the cell connected the flux chamber to the FTIR while the other inlet fed the nitrogen by-pass to the cell. The outlet was fed to a hood to exhaust the fuel vapors. The bypass flow rate was kept constant at 85 mL/min and it does not affect the fuel transport in the foam or in the flux chamber. Before each experiment, a zero fuel baseline was established to ensure that no leftover fuel or water was present in the flux chamber. Reference spectra were used to calibrate the FTIR to accurately identify the concentration of incoming gases. Reference spectra for n-heptane, iso-octane, methyl-cyclohexane, carbon dioxide, and water were used at concentrations varying from 25 ppm to 200 ppm to ensure a more accurate measurement from the FTIR. Experiments were run for roughly 2500 s to focus on the fuel flux at early timescales that would most likely relate to fuel vapor suppression during fire extinction. Because of the short timescales of the measurements, no steady state in the fuel flux through the foam is seen. Experiments were run in triplicate to calculate the average and associated error bars. We converted the measured fuel concentration to a fuel flux (moles of fuel per unit area of foam and per unit time) by multiplying the concentration with the molar flow rate (0.014 mol/min) of total nitrogen through the FTIR and dividing by the surface area of the foam layer (21.64 cm^2).

3. Results and discussion

We report FTIR data as fuel flux with time for a given fuel and surfactant formulation. In addition to the fuel flux, this data allowed us to determine the “break-through” time, which is the time it takes the fuel concentration measured by the FTIR to reach 10 ppm, for comparing fluorinated and fluorine-free foams and different fuels. The fuel flux measurements are repeated three times and the error bars represent one standard deviation in the data.

Fig. 3 shows the fuel flux through 4 cm thick foam layers of AFFF and RF6 placed on an n-heptane liquid pool at 20 °C. The fuel flux is much smaller than that (7.5e-08 mol/cm^2s) reported for an uncovered pool [4]. The current design of the flux chamber is expected to establish steady state very quickly for an uncovered n-heptane pool similar to our previous design [4] due to similar size and conditions. The steady state is achieved due to the flow of nitrogen through the porous frit disc placed 1 cm from the pool and due to the fixed vapor pressure of n-heptane at the pool surface. Williams et al. [4] reported a steady state fuel flux of 7.5e-08 mol/cm^2s for an uncovered n-heptane pool. When the foam layer is applied on top of the pool, the fuel concentration at the foam surface rises slowly over time and the fuel flux into the chamber also increases with time. The slow increase in fuel flux as measured by FTIR is shown in Fig. 3 for AFFF and RF6 foams of same thickness. The slow rise in fuel transport is indicative of the transport resistance of the foam.

Fig. 3 shows that AFFF has a lower fuel flux than RF6 by an order of magnitude over 2000 s for the same foam layer thickness over the same room temperature n-heptane fuel. The AFFF layer suppresses the fuel flux of n-heptane at the pool surface by a factor of 300 from 7.5e-8 to 2.5e-10 mol/cm^2s at 1500 s and the suppression is much greater during the initial 10 min. In comparison, the RF6 layer suppresses the n-heptane flux by a factor of 42 from 7.5e-8 to 1.8e-9 mol/cm^2s at 1500 s. The suppression factors measured during the transient period of fuel transport are much higher than the steady state values reported by Williams et al. [4]. The fuel vapor break-through times are 276 s and 820 s for RF6 and AFFF respectively and are indicated by the “break-through flux” in Fig. 3 at a flux of 1.21e-10 mol/cm^2s corresponding to 10 ppm of fuel vapor. It is difficult to distinguish the difference in the data reported by Schaefer et al. [17] between AFFF and RF6 because their experiments were run for very long time periods (350 min), where the foams collapsed due to degradation and reached a value corresponding to the bare fuel surface at about 140 and 300 min for 1 cm thick RF6 and AFFF respectively. The large difference in the measured fuel flux between AFFF and RF6 shown in Fig. 3 can be due to differences in the composition of surfactant solution and in properties of the foams listed in Table 3.

Fig. 4 compares fuel flux through a 4 cm thick AFFF foam layer over three fuels: n-heptane, iso-octane, and methyl-cyclohexane at 20 °C. In Fig. 4, AFFF has the smallest fuel flux over iso-octane, slightly greater for n-heptane, and largest for methyl-cyclohexane. The break-through times are greater than 1900 s for iso-octane, 820 s for n-heptane, and less than 80 s for methyl-cyclohexane. At 1500 s, fuel flux is 1e-11 mol/cm^2s, 2.5e-10 mol/cm^2s, and 2.4e-9 mol/cm^2s for iso-octane, n-hep-

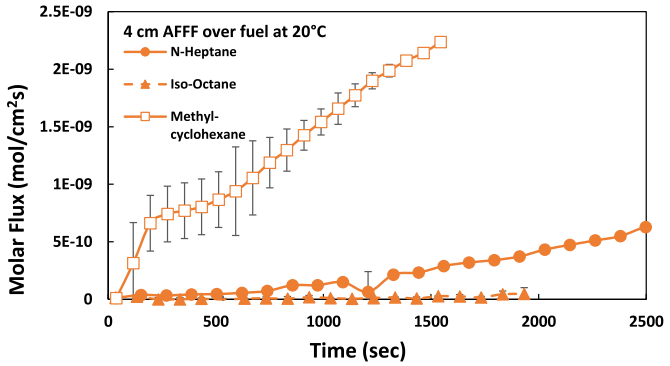

Fig. 4. AFFF, 4 cm thick foam layer covering different fuel pools at 20 °C.

tane, and methyl-cyclohexane respectively. The measurement of Williams et al. [4] also show that AFFF foam suppresses iso-octane and n-heptane fuel flux more than that of methyl-cyclohexane at steady-state achieved at high nitrogen flow rates.

One of the most interesting observations from the data shown in Fig. 4 is that the smallest molar flux through AFFF is measured over the fuel iso-octane, which is the most unyielding fuel of the three for AFFF foam solution to form an "aqueous film" because of its low surface tension as shown in Table 2. Moran et al. [8] showed that AFFF foam solution (6% FC195, 3M Co.) had either very low (0.2 dynes/cm) or negative (−1.3 dynes/cm) spreading coefficients (see Table 3 of [8]) leading to marginal or no "aqueous film" formation on an iso-octane pool. Indeed, Williams et al. [4] showed that AFFF foam solutions (6% National Foam Co, and 3% Buckeye) either did not form a film or on some attempts formed a marginal (slow spreading) film on iso-octane in a MilSpec's film and sealability test with the cyclohexane pool replaced with the fuel of interest. This means the aqueous solution that drains from AFFF foam cannot form a film over an iso-octane pool surface during our experiment. Despite the absence of a film barrier, Fig. 4 shows that very small amounts of iso-octane vapor are transported through the AFFF foam relative to n-heptane and methyl-cyclohexane, both of which enable film formation. In comparison to the iso-octane pool, AFFF foam solution was found to form an "aqueous film" easily on a methyl-cyclohexane pool [4]. Despite the film formation, methyl-cyclohexane pool exhibits the highest steady-state [4] fuel flux and transient fuel flux as shown in Fig. 4. Fig. 4 suggests that the aqueous film may be less effective than the foam layer as a barrier to fuel.

Moran et al. [8] measured fuel flux through a foam solution film covering an n-octane pool using a similar sized flux chamber as the one in our study. They used much higher flow rates (630 mL/min) through the porous disc compared to 234 mL/min used in the current study. Using a glass cup, Moran et al. [8] poured n-heptane up to the rim of the cup. The surfactant solution was applied onto the pool surface, using a pipette, which allow it to spread and form a film. The thickness of the film was then calculated from the volume pipetted to the surface and the surface area of the cup. The concentration of fuel vapors above the film was sampled using a gas chromatograph before and after the film was applied. Moran et al. plotted the results as a percent decrease of fuel vapors above the film over time. Their data showed that the n-octane vapor concentration above the aqueous film was suppressed by a factor of 50 when the estimated film thickness was 24–47 μm within the first 5–7 min after film formation; the suppression factor was smaller (factor 10) for a thinner (9 μm) film. But, after the first several minutes, the fuel vapor concentration above the film began to increase slowly and approached that of the uncovered pool, reaching 70–90% of the vapor concentration within an hour depending on the film's thickness. In comparison, the suppression of iso-octane fuel flux (1e-11 mol/cm^{2}s) shown in Fig. 4 is many times greater than 50 even after 0.5 h. This is despite the fact that iso-octane has a higher vapor pressure (40.5 mmHg) than n-octane (12.75 mmHg) at 25 °C [26]. Correcting for the vapor pressure difference between n-heptane and n-octane, we estimate the fuel flux for an uncovered n-octane pool to be 2.4e-08 mol/cm^{2}s and a suppression factor of 2400 by AFFF foam based on Fig. 4. Our transient data shows that the foam contributes greatly to the effective barrier suppressing fuel transport.

Measurements from our flux chamber and work of Moran et al. [8] has shown that the foam plays a significant role compared to "aqueous film" in blocking fuel because a 4 cm foam layer contains a myriad of aqueous lamellae and air, forming a significant barrier to fuel transport relative to a few micrometers thin, single "aqueous film". Fuel transport through the foam layer can occur as the fuel travels through the gas phase contained in the foam bubbles, through the liquid lamella (liquid layer between two adjacent bubbles or bubble wall) surrounding the bubbles, and through the plateau borders (liquid columns formed at the junction of three adjacent bubbles) as shown in Fig. 5. The vaporized fuel first dissolves into the liquid lamella. Transport through liquids is much slower than transport through gases due to differences in diffusion coefficients between gases and liquids by four orders of magnitude. Therefore, the dissolved fuel vaporizes from the lamella into a gaseous bubble in the foam. The fuel vapor then re-dissolves into another liquid lamella further up the foam layer and continues this transport until the vapor has reached the foam layer surface as depicted in Fig. 5.

The foam solution composition may affect fuel transport since AFFF has both fluorocarbon and hydrocarbon surfactants and RF6 has only the hydrocarbon surfactants. All surfactants adsorb at the lamella interface (bubble surface) as shown by the individual lamella diagrams in Fig. 5, which only shows fluorocarbon surfactant versus hydrocarbon surfactant absorption at the lamella interface for emphasis. Fluorocarbon surfactants in AFFF are unique in having both hydrophobic and oleophobic repulsions. The surfactant repels a hydrocarbon fuel like n-heptane and suppress fuel dissolution into the liquid lamella as depicted by the lamella diagram in Fig. 5. The fluorocarbon surfactant may impede the transport through the foam layer. RF6

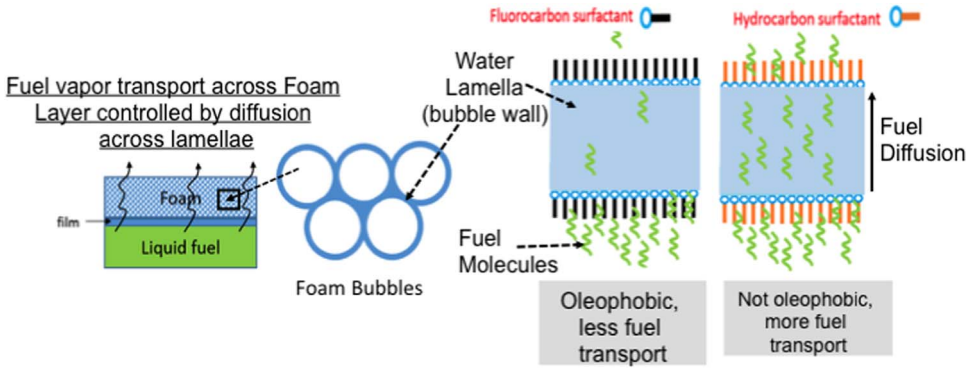

Fig. 5. Fuel transport within the bubble structure and the lamellae, and the role of fluorocarbon and hydrocarbon surfactants in the transport across a lamella.

contains hydrocarbon surfactants which are also hydrophobic, but the hydrocarbon tails do not repel the hydrocarbon fuel and are not as oleophobic as fluorocarbon surfactants. Fuel vapors can easily dissolve into the liquid lamella and move unimpeded by the hydrocarbon surfactant of RF6 through the foam layer resulting in faster transport in RF6 foam compared to AFFF as shown in Fig. 5. In addition to repulsion towards fuel, foam stability and lamella thickness are also important to reduce fuel flux through the lamellae. Surfactants can affect the thinning dynamics of lamellae, thereby affecting foam degradation directly [25]. A synergy between the fluorocarbon and hydrocarbon surfactants contained in AFFF was shown to be important for forming stable foams, despite reduced repulsion towards fuel by the presence of hydrocarbon surfactants in the AFFF formulation [27]. Therefore, a balance between foam stability and oleophobicity appears to exist and affects fuel transport through AFFF.

The basis for the proposed mechanism shown in Fig. 5 is the distinguishing feature that the tail of a fluorocarbon surfactant in AFFF foam solution interacts less favorably with fuel compared to a hydrocarbon surfactant in RF6 foam solution. This distinguishing interaction may be related to the solubility of a fuel in a surfactant solution with/without a fluorocarbon surfactant. To investigate this, we measured fuel solubility in a 1.3% Triton X-100 (a hydrocarbon surfactant, Sigma Aldrich) aqueous solution and in an aqueous solution containing a mixture of 0.3% Capstone (a 27% fluorocarbon surfactant solution, DuPont Inc.) and 0.1% Triton X-100. The surfactant concentrations correspond to twice their critical micelle concentrations (CMC, 0.62% for Triton X-100% and 0.23% for a 3:1 mixture of Capstone and Triton X-100 in distilled water), which we determined by measuring dynamic surface tension in a bubble tensiometer; above CMC, surface tension becomes independent of surfactant concentration. A vial of 10 mL of the surfactant solution and 5 mL of fuel were mixed vigorously by hand for 30 s to saturate both fuel and aqueous phases. The vial was then placed in a centrifuge at a low rpm of 4000 for 15 min to separate the phases. The aqueous phase was extracted and fuel solubility was analyzed via GC-MS using an Agilent 7890 A gas chromatograph coupled with an Agilent 5975 C mass spectrometer (MS) detector operating in electron ionization mode and an Agilent 7693 A auto-injector. Fuel concentrations were determined using selective ion monitoring (SIM) for increased sensitivity and an internal standard method using iso-octane or methyl-cyclohexane as the internal standards.

Chromatographs of the solubility's for three fuels in the two foam solutions are shown in Figs. 6–8. Different internal standards were used in each figure. In each figure, we superimposed the two chromatographs for the aqueous samples with and without the fluorocarbon surfactant (Capstone). The solid line represents the foam solution with Capstone and the broken line without. Fig. 6 shows that the methyl-cyclohexane is suppressed by the presence of Capstone as indicated by the absence of a peak at a retention time of 3.65 min while a significant peak appears in the foam solution without Capstone. The inset in the figure shows an extremely small peak for the fuel in the foam solution containing Capstone. Figs. 7 and 8 show similar results for n-heptane and iso-octane respectively. Figs. 6–8 suggest that when fuel molecules approach a bubble lamella containing a fluorocarbon surfactant, it can repel fuel adsorption into the lamella and the bubble and by extension into the foam, consistent with the smaller fuel transport rates shown in Fig. 3 for AFFF relative to RF6.

The mechanism depicted in Fig. 5 is supported by our fuel flux data for different fuels shown in Fig. 4 and in solubility data collected in Figs. 6–8. As mentioned before, the fuel vapor travels through the foam layer by dissolving into the liquid lamella of the foam. Although the three fuels compared in this paper have similar vapor pressures, they differ in their solubility with water as seen in Table 2. Iso-octane and n-heptane have similar solubility in water, with n-heptane having the slightly higher solubility in water than iso-octane. Methyl-cyclohexane is an order of magnitude more soluble in water than the other two fuels. A lower solubility indicates less fuel has dissolved into an aqueous solution compared to higher solubility. If less fuel dissolves into the liquid lamella, less fuel will diffuse through the foam, decreasing the concentration of fuel across the foam thickness, decreasing the observed fuel flux. Iso-octane has the smallest solubility in water meaning less fuel would dissolve into the liquid lamella compared to n-heptane and methyl-cyclohexane. This smaller concentration of fuel would decrease the fuel flux. The trend seen in the solubility of fuels in water follows the trend seen in Fig. 4 of higher fuel flux as the fuel solubility increases. However, the solubility data provided in Table 2 is for fuel dissolving into water, which is 98% of the foam solution, but the type of surfactant affects the solubility of the fuel in the foam solution [28] as shown in Figs. 6–8. The transient fuel flux data suggests that a key to lowering the fuel flux through foam is focusing on the adsorption/solubility of fuel vapors at a lamella surface and the transport rate of fuel through a lamella. The effects of foam degradation by lamella thinning were minimized in our experiments, but can have a significant effect on transport in fire extinction conditions and could be influenced by the surfactant.

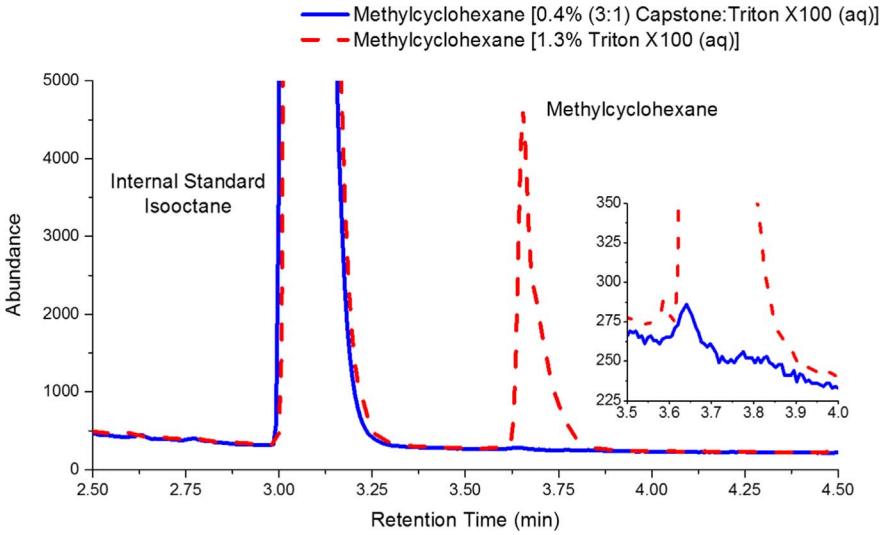

Fig. 6. Solubility of methyl-cyclohexane in aqueous solution of Triton X-100 hydrocarbon surfactant with and without the fluorocarbon surfactant solution, Capstone, at twice their respective CMC values. The inset figure shows the magnified signal for fuel in solution with Capstone.

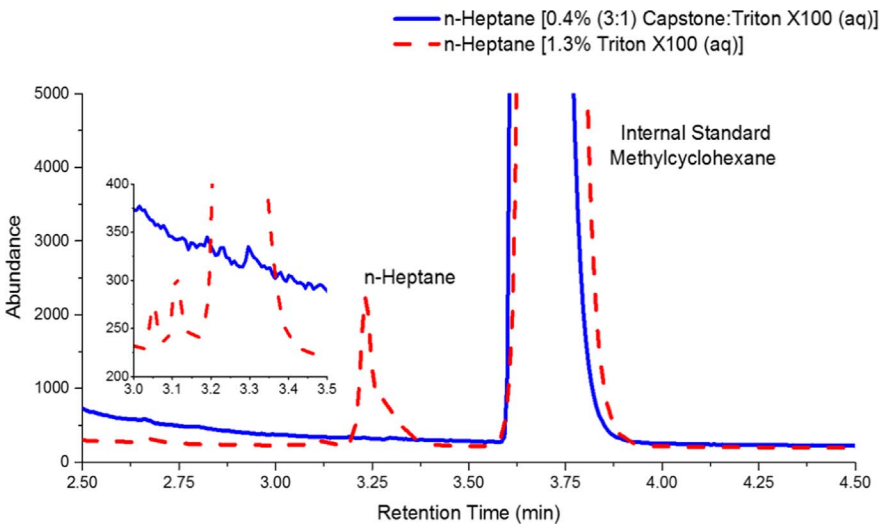

Fig. 7. Solubility of n-heptane in aqueous solution of Triton X-100 hydrocarbon surfactant with and without the fluorocarbon surfactant solution, Capstone, at twice their respective CMC values.

4. Conclusions

We designed a flux chamber to measure the initial transient fuel flux for AFFF and RF6 foam layers covering a fuel pool before significant degradation of the foam occurred. We characterized the intrinsic differences in the dynamics of fuel transport through the two foams generated using the same sparging method with different surfactant formulations contained in the foams. AFFF contains fluorocarbon surfactants while RF6 is fluorine-free. AFFF has an order of magnitude lower fuel flux and a break-through time three times greater than RF6. The transient flux measurements were performed at ambient conditions in the absence of a fire without significant foam degradation, which should be considered in future work to find fluorine-free surfactants and foams with improved fire suppression.

AFFF had the lowest fuel flux over iso-octane with a break-through fuel vapor time over 1900 s, the second slowest fuel flux over n-heptane with a break-through fuel vapor time of 820 s, and the fastest flux over methyl-cyclohexane with a break-through time under 80 s. This result was surprising since AFFF is unable to form a film over iso-octane because of the low surface tension of the fuel. The lowest measured fuel flux was seen in the absence of film formation and the highest was seen when the film formation and spreading was fast due to the high surface tension of the methyl-cyclohexane fuel pool. The transient fuel flux data for AFFF covering different fuel pools show that the foam layer is a very effective barrier to fuel transport. These data are insufficient to conclude that the “aqueous film” has no role in fire suppression, but the data suggest that improving foam properties can lead to more effective suppression of fuel transport using fluorine-free surfactants that lack “aqueous film formation”.

We propose that an important barrier to fuel transport in the foam is the role of the surfactant in bubble lamellae. Fuel vapors absorbed into the liquid lamella may be impeded by the surfactant adsorbed at the lamella interface. AFFF contains fluorocarbon surfactants that are hydrophobic and strongly oleophobic. RF6 contains hydrocarbon surfactants, which have hydrocarbon tails similar to fuels, which are less oleophobic than fluorocarbon surfactants. Furthermore, solubility of the fuel in the foam solution was found to be less with fluorocarbon surfactants than with hydrocarbon surfactants alone resulting in its faster fuel flux through the fluorine-free foam. Future research aimed at finding an environmentally friendly alternative to AFFF may want to target surfactants that result in increased repulsions toward fuel and reduced absorption at lamella surfaces to mimic a fluorocarbon surfactant's effect on the fuel transport. In addition, foam degradation, liquid drainage, bubble coarsening/rupture, can also be affected by fuel and the surfactant, and should be considered for improving fire suppression with fluorine-free foams. Experiments and computational

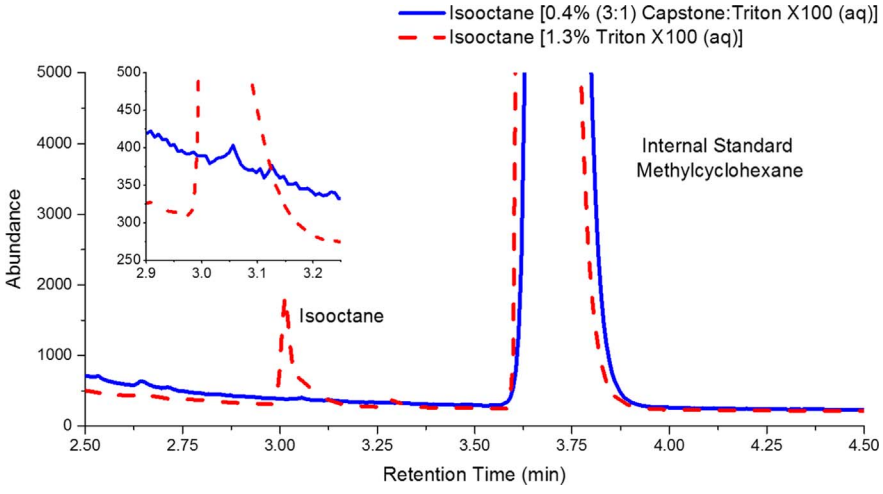

Fig. 8. Solubility of iso-octane in aqueous solution of Triton X-100 hydrocarbon surfactant with and without the fluorocarbon surfactant solution, Capstone, at twice their respective CMC values.

models to understand lamella thinning and fuel transport through a single lamella will potentially lead to significant insights for finding environmentally benign fluorine-free surfactants with requisite fire suppression.

Acknowledgements

We would like to acknowledge Dr. M.W. Conroy, Dr. Bradley Williams, and Dr. James W. Fleming, formerly of the Naval Research Laboratory, for their expertise and advice. We also thank the Office of Naval Research for supporting this work through the Naval Research Laboratory.

References

[1] R. Sheinson, B. Williams, C. Green, J. Fleming, R. Anleitner, S. Ayers, A. Maranghides, The future of aqueous film forming foam (AFFF): performance parameters and requirements, Proceedings of the 12th Halon Options Technical Working Conference, Albuquerque, NM, 2002.
[2] Military Specification: Fire Extinguishment Agent. Aqueous Film-Forming Foam (AFFF) Liquid Concentrate, For Fresh and Sea Water, MIL-F-24385F, Naval Sea System Command, 1992.
[3] S. Zhang, D.N. Lerner, Review of physical and chemical properties of perfluorooctanyl sulphonate (PFOS) with respect to its potential contamination on the environment, Adv. Mater. Res. 518–523 (2012) 2183–2191.
[4] B. Williams, C. Butterworth, Z. Burger, R. Sheinson, J. Fleming, C. Whitehurst, J. Farley, Extinguishment and burnback tests of fluorinated and fluorine-free fire-fighting foams with and without film formation, Suppression, Detection, and Signaling Research and Applications – A Technical Working Conference, NFPA, Orlando, FL, 2011.
[5] J. Scheffey, R.L. Darwin, J.T. Leonard, Improved fire protection for flight deck weapons staging area (Bomb Farm), Naval Research Laboratory Memo Report 5917, Washington DC, 1987.
[6] B. Lattimer, C. Hanauska, J. Scheffey, F. Williams, The use of small-scale test data to characterize some aspects of firefighting foam for suppression modeling, Fire Saf. J. 38 (2003) 117–146.
[7] M.K. Bernett, L.A. Halper, N.L. Jarvis, T.M. Thomas, Effect of adsorbed monomolecular films on the evaporation of volatile organic liquids, IEC Fundam. 9 (1970) 150–156.
[8] H.E. Moran, J.C. Burnett, J.T. Leonard, Suppression of fuel evaporation by aqueous films of fluorochemical surfactant solutions, Naval Research Laboratory Memo Report 7247, Washington DC, 1971.
[9] T. Schaefer, B.Z. Dlugogorski, E.M. Kennedy, Sealability properties of fluorine-free fire-fighting foams (FfreeF), Fire Technol. 44 (2008) 297–309.
[10] R. Hetzer, F. Kümmerlen, The Extinguishment Performance of Experimental Siloxane-Based AFFF, Interflam 2016, Royal Holloway College, Egham, 2016.
[11] G.B. Greyer, Firefighting effectiveness of aqueous-film-forming-foam (AFFF) agents, National Aviation Facilities Experimental Center, FAA-NA-72-48, 1973.
[12] H.W. Carhart, J.T. Leonard, R.L. Darwin, R.E. Burns, J.T. Hughes, E.J. Jablonski, Aircraft carrier flight deck fire fighting tactics and equipment evaluation tests, Naval Research Laboratory Memo Report 5952, Washington DC, 1987.
[13] H.L. Hardy, C.J. Purnell, Use of foam for emergency suppression of vapor emissions from organic isocyanate liquid surfaces, Am. Oxxup. Hyg. 21 (1978) 95–98.
[14] J.A. Pignato Jr., Evaluation test for foam agent effectiveness, Fire Eng. (1984) 46–48.
[15] C.P. Hanauska, The Suppression of Vapors from Flammable Liquids with Stabilized Foams (Masters Thesis), Worcester Polytechnic Institute, 1988.
[16] M.L. Carruette, H. Persson, M. Pabon, Additive for low viscosity of AFFF/AR concentrates – study of the potential fire performance, Fire Technol. 40 (2001) 367–384.
[17] T.H. Schaefer, B.Z. Dlugogorski, E.M. Kennedy Vapour suppression of n-heptane with fire fighting foams using laboratory flux chamber, 7th Asia-Oceania Symposium on Fire Science and Technology, 2007.
[18] B.Z. Dlugogorski, S. Phiyanalinmat, E.M. Kennedy, Dynamic surface and interfacial tension of afff and fluorine-free class b foam solutions, Fire Safety ScienceProceedings of the 8th International Symposium, pg. 719–730, 2005.
[19] ScienceLab.com, 2,2,4-Trimethylpentane [Data File], 2016, Retrieved from ⟨https://www.sciencelab.com/msds.php?MsdsId=9927418⟩, (2013).
[20] ScienceLab.com, N-heptane [Data File], 2016, Retrieved from ⟨http://www.sciencelab.com/msds.php?MsdsId=9924237⟩, (2013).
[21] ScienceLab.com, Methylcyclohexane [Data File], 2016, Retrieved from ⟨https://www.sciencelab.com/msds.php?MsdsId=9924678⟩, (2013).
[22] Royal Society of Chemistry, Substance: 2,2,4-Trimethylpentane [Data File], 2016, Retrieved from ⟨http://www.rsc.org/learn-chemistry/wiki/Substance:2,2,4-Trimethylpentane⟩, (2011).
[23] Royal Society of Chemistry, Substance: Heptane [Data File], 2016, Retrieved from ⟨http://www.rsc.org/learn-chemistry/wiki/N-HEPTANE⟩ (2011).
[24] Royal Society of Chemistry, Substance: Methylcyclohexane [Data File], 2016, Retrieved from ⟨http://www.rsc.org/learn-chemistry/wiki/Methylcyclohexane⟩, (2011).
[25] K.M. Hinnant, M.W. Conroy, R. Ananth, Influence of fuel on foam degradation for fluorinated and fluorine-free foams, Colloids Surf. A 522 (5) (2017) 1–17 (Submitted).
[26] Royal Society of Chemistry, Substnace: n-octane [Data File], 2011.
[27] K. Osei-Bonsu, N. Shokri, P. Grassia, Foam stability in the presence and absence of hydrocarbons: from bubble- to bulk-scale, Colloids Surf. A: Physicochem. Eng. Asp. 481 (2015) 514–526.
[28] Y. An, S. Jeong, Interactions of perfluorinated surfactant with polycyclic aromatic hydrocarbons: critical micelle concentration and solubility enhancement measurements, Colloid Interface Sci. 242 (2001) 419–424.